SCIENCE CHINA
Earth Sciences

• RESEARCH PAPER •

January 2018 Vol.61 No.1: 33–46
https://doi.org/10.1007/s11430-017-9099-0

Atmospheric environmental capacity and urban atmospheric load in mainland China

XU DaHai[1*], WANG Yu[1] & ZHU Rong[2]

[1] *State Key Laboratory of Severe Weather & Key Laboratory of Atmospheric Chemistry of CMA, Chinese Academy of Meteorological Sciences, Beijing 100081, China;*
[2] *National Climatic Center, Beijing 100081, China*

Received April 19, 2017; accepted August 18, 2017; published online November 15, 2017

Abstract Daily and annual average atmospheric environmental capacity coefficient (*A*-value) sequences for mainland China are calculated from hourly data recorded at 378 ground stations over 1975–2014. *A*-values at different recurrence intervals are calculated by fitting the sequences to Pearson type III distribution curves. Based on these *A*-values and source-sink balance (reference concentration 100 μg m^{-3}), atmospheric environmental capacities at the recurrence intervals are calculated for all of mainland China and each provincial administrative region. The climate average atmospheric environmental capacity reference value for the entire mainland is 2.169×10^7 t yr^{-1}. An urban atmospheric load index is defined for analyses of the impact of population density on the urban atmospheric environment. Analyses suggest that this index is also useful for differentiating whether air quality changes are attributable to varying meteorological conditions or variations of artificial emission rate. Equations guiding the control of unorganized emission sources are derived for preventing air quality deterioration during urban expansion and population concentration.

Keywords Atmospheric environmental capacity, Pearson type III distribution, Recurrence interval, Urban atmospheric load index, Emission rate density

Citation: Xu D H, Wang Y, Zhu R. 2018. Atmospheric environmental capacity and urban atmospheric load in mainland China. Science China Earth Sciences, 61: 33–46, https://doi.org/10.1007/s11430-017-9099-0

1. Introduction

Atmospheric environmental capacities on a large scale and allowable emissions on the local scale are critical parameters supporting regional atmospheric environment management. The former aim to prevent regional accumulation of pollutants and the latter help ensure that monitored pollutant concentrations are below permissible levels (Xu and Wang, 2013). The present study is focused on methods for determining atmospheric environmental capacities and their statistical characteristic values. Determination of these properties can provide basic information guiding regional emission management and urban agglomeration planning, although this has been a challenging task.

Several studies (Sun et al., 2015; Xue et al., 2014; Qian and Wang, 2011; Li et al., 2010; Xu et al., 2010; Xiao et al., 2008; An et al., 2004) have calculated atmospheric environmental capacities by multi-source modeling, based on emission inventories and optimization of maximum total emission, under the criterion that target pollutant concentrations at monitoring sites meet national standards. A major advantage of this approach is that the calculated atmospheric environmental capacities are directly linked to environmental quality standards and can thereby facilitate emission regulation. In using this modeling approach to determine the statistical parameters of atmospheric environment capacity while considering the statistical aspects of meteorological conditions, the model involves statistical characteristics of the sampling population

* Corresponding author (email: xudh2013@qq.com)

© Science China Press and Springer-Verlag GmbH Germany 2017

of sources, which vary by period. In fact, in this modeling, these basic information are usually established with reference meteorological conditions and emission source scenarios. As a result, the reliability of the statistical characteristics of calculated environmental capacity is unclear. Furthermore, because this approach considers emissions while ignoring pollutant removal-accumulation processes in an entire region, it essentially calculates the total permissible emission under given scenarios.

Atmospheric environmental capacity expresses the balance between pollutant emission and removal at specified pollutant concentrations. We recently (Xu and Wang, 2013; Xu et al., 2016) defined atmospheric environmental capacity as follows. For a given volume in atmosphere and time interval, when pollutant generation (source) and removal (sink) reach a balance, the pollutant concentration maintains a specified value (threshold concentration), and the rate of pollutant generation (emission) is defined as the atmospheric environmental capacity under the threshold concentration. According to this concept, the determination of atmospheric environmental capacity is transformed into ascertaining the rate of pollutant removal in the atmospheric volume at a given threshold concentration. This approach offers several advantages. For example, the capacity determined is mainly dependent on natural conditions and independent of the properties of emission sources. Moreover, the data examined represent a relatively homogeneous population with relatively stable statistical aspects, and the related frequency curves are readily fit to theoretical distributions. A disadvantage of this approach, however, is that the determined capacity is not directly linked to pollutant concentrations at monitoring sites. Thus, the permissible emission for each source must be further calculated by multi-source modeling. Despite this, when the permissible total emission is set to less than the atmospheric environmental capacity determined by this approach, pollutant accumulation is impossible because of the principle of source-sink equilibrium. Therefore, the Chinese national standard for atmospheric environmental capacity determination (GB/T 3840-91: Technical method for making local emission standards of air pollutants) lists this approach as the atmospheric environmental capacity coefficient method (frequently called the *A*-value method).

Natural removal of pollutants in the atmosphere proceeds through chemical conversion to secondary pollutants and transport via physical processes (e.g., advection, turbulent diffusion, and dry/wet deposition). The *A*-value method ignores pollutant removal via chemical conversion. For primary pollutants, the capacity obtained is only an ideal physical capacity, which must not be greater than the "real" capacity when chemical conversion is included. For secondary pollutants, there is a chemical process for the generated items, and only the physical removal process for the purge items. Therefore, the physical capacity of secondary pollution obtained by the *A*-value method should be closer to the "true" capacity, unless there is a further chemical removal process.

In this study, we investigated the rate of pollutant removal in the atmosphere of mainland China via physical processes (hereafter called the removal rate) by the *A*-value method, assuming homogeneous pollutant distribution in the atmospheric boundary layer at a reference concentration (C_r) of 100 μg m^{-3}. We also calculated removal rates at various recurrence intervals in provincial-level administrative regions, and correspondingly estimated ideal atmospheric environmental capacities for several pollutants (hereafter called atmospheric environmental capacities). Finally, we analyzed the effect of urban scale on pollutant removal rate for the local atmosphere, addressed the load on the atmospheric environment caused by urban expansion and population agglomeration, and developed an indicator for identifying factors responsible for changes of urban air quality (i.e., emission vs. meteorological conditions).

2. Data and methods

2.1 Data

Hourly data recorded by ground stations over 1975–2014 were obtained from the Information Center of China Meteorological Administration. After screening for data consistency and completeness, data from 378 stations (Figure 1) were used.

2.2 Methods

During self-purification in the atmosphere, primary pollutants can partially be chemically converted to fine particles. Ozone may also be produced. Therefore, chemical conversion is typically not a complete pollutant removal process. A recent study (Xu et al., 2016) analyzed pollutant removal via physical processes, proposing that when emissions (source) and self-purification (sink) proceed simultaneously, pollutant concentration temporal variation in the atmosphere is described by

$$\bar{c} = \frac{q}{A \times \sqrt{S}} \times \left(1 - \mathrm{e}^{-\frac{A}{H \times \sqrt{S}} \times t}\right) + \bar{c}_0 \, \mathrm{e}^{-\frac{A}{H \times \sqrt{S}} \times t}, \tag{1}$$

where, t is the time variable and

$$A = 0.0031536 \times \frac{\sqrt{\pi} \times U \times H}{2} \times \left(1 + \frac{2 \times \sqrt{S} \times (v_d + w_r \times R)}{\sqrt{\pi} \times U \times H} \times 10^3\right). \tag{2}$$

In eq. (2), A is the atmospheric environmental coefficient (A-value, 10^4 km^2 yr^{-1}) representing physical self-purification of the atmosphere, q (10^4 t yr^{-1}) is the pollutant emission rate,

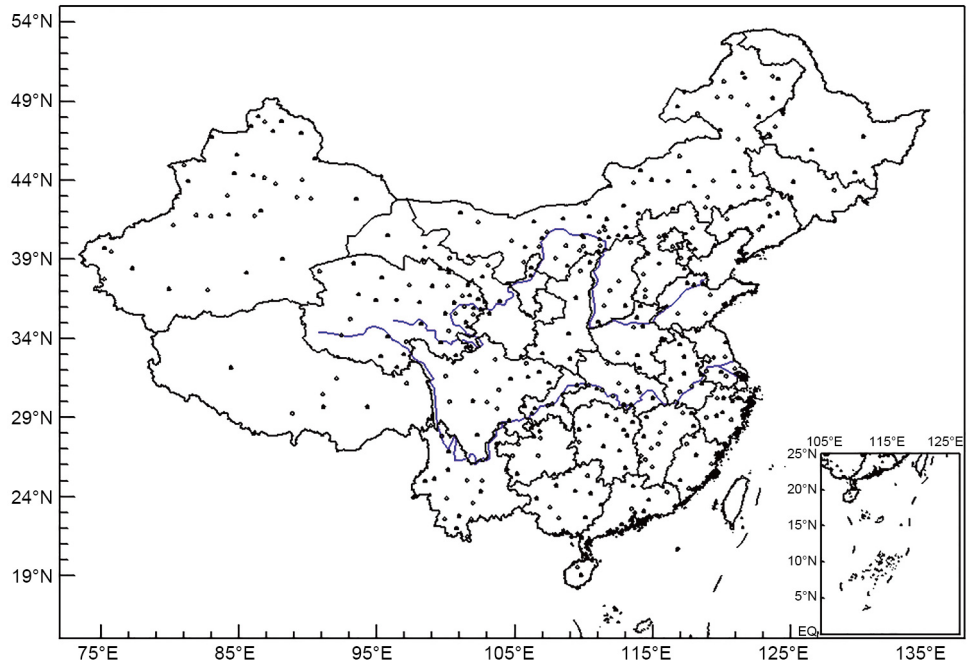

Figure 1 Distribution of ground stations whose data were used.

$\bar{c}$ (in mg m^{-3}) is average concentration of the pollutant, S (km^2) is the area of the region in question, U (m s^{-1}) is the sum of the speeds of advection and pseudo-diffusion, H (m) is thickness of the atmospheric boundary layer (Xu, 1987; Zilitinkevich, 1972) calculated following a Chinese national standard (GB/T3804-91, Supplement E-E1), v_d (m s^{-1}; value range in Li et al., 1985) is the dry deposition speed defined as the ratio between dry deposition flux and concentration (Chamberlain, 1953), and w_r (dimensionless; w_r=1.9×10^{-5} when annual precipitation R is expressed in mm a^{-1}) is the washout ratio (Xu and Zhu, 1989).

The washout effect of precipitation is represented by the wet deposition rate v_w, and v_w=w_r×R. On the spatial scale of cities, airflow is a dominant factor determining the A-value.

When q=0 (absence of pollutant emission), eq. (1) becomes

$$\bar{c} = \bar{c}_0 \, \mathrm{e}^{-\frac{A}{H\times\sqrt{S}}\times t} = \bar{c}_0 \, \mathrm{e}^{-\frac{t}{T}}, \tag{3}$$

where $T = H\times\sqrt{S}/A$ is the decay time scale.

Additionally, when S is expressed in m^2, A in m^2 s^{-1}, and q in mg s^{-1}, eq. (2) can be rewritten as

$$A = \frac{\sqrt{\pi}\times U\times H}{2} + (v_d + v_w)\sqrt{S}. \tag{4}$$

From the latter part of eq. (3), we can write:

$$\frac{\sqrt{\pi}\times U}{2\sqrt{S}} + \frac{v_d + v_w}{H} = \frac{1}{T}. \tag{5}$$

When the equivalent diameter of the region L ($L = 2\sqrt{S/\pi}$) is used as its characteristic dimension, the first term on the left half of eq. (5) can be rewritten as $1/T_L = U/L$, where T_L represents a characteristic time (i.e., the time required to travel a distance of L at velocity U). Let $T_h = H/(v_d + v_w)$, where T_h represents another characteristic time (i.e., the time required to penetrate the thickness of the atmospheric boundary layer at the sum of the dry and wet deposition speeds). Then, eq. (5) can be simplified as

$$\frac{1}{T} = \frac{1}{T_L} + \frac{1}{T_h}. \tag{6}$$

On the spatial scale of a city, T is mainly determined by T_L. Consequently, the shortest decay time (fastest transport of pollutants out of the city by advection) is obtained when the shortest dimension of the city is along the prevailing wind direction. Furthermore, we should also note that an expansion of a city will enlarge its equivalent diameter and increase the characteristic decay time for atmospheric pollutants proportionally.

When the removal rate of a pollutant and its emission rate are in equilibrium, they are equal in magnitude. Thus, in eq. (1), we let $\bar{c} = c_r$ and $t\to\infty$, so the equation becomes

$$q = C_r \times A \times \sqrt{S}, \tag{7}$$

where q is the removal rate in the region examined.

We define removal rate density Q_d as the removal rate per unit area:

$$Q_d = \frac{A\times C_r}{\sqrt{S}}. \tag{8}$$

Q_d essentially describes the intensity of pollutant generation and removal of the area source (sink). If region S includes multiple sub-regions (denoted S_i) whose maximum permissible pollutant concentration in each is c_i, then according to the Chinese standard (GB/T3840-91), q_i in S_i is $q_i = A\times c_i \times S_i/\sqrt{S}$. Additionally, if each S_i has a unique

A-value but identical C_r, we can similarly write (Xu et al., 1990):

$$q_i = A_i \times C_r \times S_i / \sqrt{S}. \quad (9)$$

We used eq. (9) to calculate atmospheric environmental capacities of S, including multiple S_i with different A-values.

3. Annual removal rates in mainland China at different recurrence intervals

3.1 Annual average A-value distribution: topography and applications

Hourly data recorded by the 378 stations (Figure 1) during 1975–2014 were used to calculate hourly, daily, and annual average A-values. Then, A-values at recurrence intervals 5, 10, 20, 30, and 100 yr were obtained by fitting to a Pearson type III distribution (Xu et al., 2016).

An A-value at a recurrence interval is defined as follows. (1) Let the average A-value in an interval $\overline{A} = a$. (2) During sampling of this interval, the probability of occurrence of an event $\{a \le a_p\}$ is denoted as $p\{a \le a_p\}$. (3) Then, the reciprocal of this probability ($T = 1/p\{a \le a_p\}$), representing the average period between two consecutive events, is defined as the recurrence interval T. Accordingly, a_p is defined as the A-value at recurrence interval T.

Mainland China is prone to pollution during autumn and winter, and sustained severe pollution is frequent from November through February. The A-value distribution was calculated for this period. For brevity, we show the climatic average A-value distribution (1975–2014; Figure 2a), A-value distribution at 5-year recurrence interval (Figure 2b), climate averaged A-value distribution for pollution-prone seasons (November–February; Figure 2c), and A-value distribution for pollution-prone seasons at 5-year recurrence interval (Figure 2d). The following trends were observed from the results.

First, in most parts of mainland China, the climate averaged A-value was 2–10 (Figure 2a), generally consistent with data listed in the Chinese standard GB/T3840-91, which was published in 1991 and drafted based on data recorded over 1950–1980. Nevertheless, there were some departures in a few regions. A-values >10 were found in southwestern Qinghai (Figure 2a), because complete climatologic data were not available for this plateau region during creation of the standard. A-values listed in the standard for Xinjiang were greater than calculated values, for reasons other than technical issues. Moreover, A-values along a line from the coastal areas to the south flank of the Nanling Mountains to a large part of Yunnan Province were larger than those in the standard, likely because our study considered dry/wet deposition and the region has substantial vegetation cover and precipitation. Aside from these discrepancies, values in Figure 2a generally match the standard, indicating that climatological conditions (i.e., determinants of atmospheric self-purification) had remained

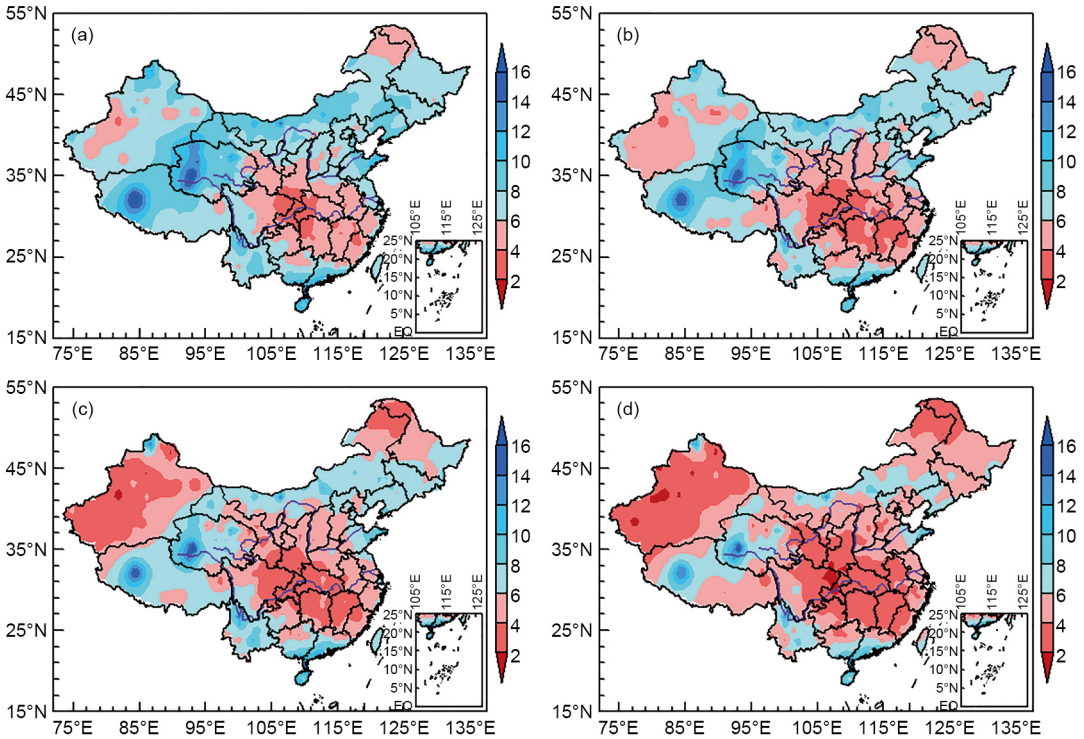

Figure 2 The distribution of A values for different recurrence interval. (a) Climate average, (b) average at 5-year recurrence interval, (c) climate average during pollution-prone seasons, (d) average at 5-year recurrence interval during pollution-prone seasons).

stable since the 1950s. Furthermore, the results show that the A-value as an indicator of atmospheric self-purification is statistically stable.

Subsequently, by area-weighted averaging, the national average A-value for mainland China was found to be 6.8, and the annual average at 5-year recurrence interval was 5.9. Then, regions with values above or below the national average were regarded as high- and low-value regions, respectively. Low-value regions, for either climate average (Figure 2a) or 5-year recurrence interval (Figure 2b), were in southeastern China, consistent with the relative humidity pattern and population distribution. This consistency occurred in these regions because they feature smooth airflow exchange, can readily retain atmospheric moisture and heat, and have abundant vegetation. For the pollution-prone seasons (Figure 2c and d), the national climatic average A-value was 5.4 and the average value at 5-year interval was 4.5, representing 21% and 24% reductions over averages for the entire year, respectively. This indicates that to maintain annual average air quality in autumn and winter, the permissible emission rate during those seasons should be reduced proportionally. Furthermore, the results (Figure 2c) also reveal that densely populated cities with A-values <6 were locations where severe atmospheric pollution events were frequent during autumn and winter.

Finally, regions with the weakest atmospheric self-purification were in the wind shadow zone on the east side of the Tibetan Plateau (Figure 2a), including eastern Sichuan, southern Gansu, southern Shaanxi, western Hunan, and western Hubei provinces. The west side of the hilly areas in southeastern China and north side of the Nanling Mountains were also low A-value regions. For these regions to maintain national average air quality, their permissible emission rates must be lower than the national average by at least 50%. In comparison, high A-value regions (Figure 2a) were along a line from the Tibetan Plateau to northern Gansu Province, Inner Mongolia, and northeast plain. A-values in these regions were 8–14, larger than the national average by approximately 50% to 100%. Furthermore, high A-value regions with optimal economic implications were along the east coast, including parts of Guangdong, Guangxi, Zhejiang, Shandong, and Liaoning provinces. Pollutant removal rates there were nearly twice the national average. Favorable atmospheric environment conditions combined with abundant regional resources, these regions possess ideal qualities for economic development.

3.2 Estimation of annual removal rates at different recurrence intervals

Removal rates for regions (each with a unique A-value) spanning a large area were calculated by eq. (9) using A-values recorded by ground stations (A_i) and area represented by each station (S_i). The reference annual average maximum permissible pollutant concentration (C_r) was taken as 100 μg m^{-3}. Table 1 lists the calculated annual removal rates.

When SO_2 was selected as the target pollutant and the permissible annual average concentration in national standard GB3095-2012 was 60 μg m^{-3}, the climatic average annual removal rates were (60/100) of the values listed in Table 1. For this target pollutant, the nationwide climatic average annual removal rate was determined by $2.169\times10^7\times0.6=1.302\times10^7$ t yr^{-1}. Similarly, using annual average standard concentration limits of several other pollutants (NO_2, NO_x, PM_{10}, $PM_{2.5}$, and NH_3), their climate average environmental capacities and recurrence-interval capacities were calculated (Table 2). Of these, according to the previous industry standard HJ/T 2.2-93 (1993), the annual average concentration threshold for NH_3 was selected as 12% of the once-sampling concentration standard (200 μg m^{-3}).

Xue et al. (2014) studied the atmospheric environmental capacities of several major pollutants in mainland China using multi-source chemical model WRF-CAMx simulation, combined with optimization of emission reduction under the constraint of annual average $PM_{2.5}$ concentrations of 333 cities meeting the national standard (GB3095-2012). Using hourly data recorded in January, April, July, and October 2010, They found the nationwide atmospheric environmental capacities to be 1.36326×10^7 t yr^{-1} for SO_2, 1.25848×10^7 t yr^{-1} for NO_x, 6.1904×10^6 t yr^{-1} for primary $PM_{2.5}$, and 6.2771×10^6 t yr^{-1} for NH_3. Compared with their results (obtained considering chemical conversion and the constraint that secondary pollutants meet the standard), our calculated capacities (Table 2, climate average) for most primary pollutants (with the exception of $PM_{2.5}$) were moderately smaller. This difference appears consistent with the fact that Xue et al. (2014) considered chemical conversion, which increased the capacities of some precursor pollutants. Moreover, different pollutants are associated with different deposition parameters, but this difference was ignored in our study because of a lack of accurate data. Nevertheless, in the calculation of environmental capacities, the contribution of deposition is typically substantially smaller than that of atmospheric ventilation. Therefore, the results of the present study are considered reliable.

Considering the notable difference in economic development between eastern and western China, it was necessary to investigate separately the atmospheric environmental capacities of eastern China. By simply ignoring data (Table 1) for western China (Tibet, Gansu, Qinghai, Ningxia, Xinjiang, Inner Mongolia, Guizhou, and Yunnan), the overall removal rate for eastern China was calculated at 7.5488×10^6 t yr^{-1}. Removal rates in eastern provinces were also calculated (Table 3), assuming that pollutant emission in western China above has no (or negligible) impact on eastern China. Under this assumption, the overall removal rate of eastern China was 1.2107×10^7 t yr^{-1}, or 56% of the nationwide value. More-

Table 1 Annual atmospheric pollutant removal rates (10^4 t yr^{-1}) in administrative regions of mainland China[a)]

Recurrence interval (a)	Climate average	5	10	20	30	100
Beijing	3.44	3.11	3.04	2.93	2.77	2.69
Tianjin	3.44	2.99	2.88	2.71	2.46	2.34
Hebei	38.13	34.17	33.39	31.99	29.82	28.93
Shanxi	32.17	28.22	27.43	26.41	24.9	24.12
Inner Mongolia	302.24	276.59	271.32	263.21	251.07	245.66
Liaoning	42.3	39.05	38.15	36.7	34.43	33.46
Jilin	45.42	40.49	39.51	37.83	35.18	34.08
Heilongjiang	104.37	91.12	88.43	84.69	79.12	76.41
Shanghai	1.71	1.51	1.47	1.42	1.35	1.31
Jiangsu	21.42	18.75	18.94	18.15	16.75	17.39
Zhejiang	23.26	21.58	21.26	20.53	19.33	18.98
Anhui	23.74	19.97	19.3	18.08	16.21	15.51
Fujian	18.01	15.8	15.36	14.67	13.65	13.17
Jiangxi	20.9	17.58	16.88	15.93	14.55	13.86
Shandong	49.4	43.76	42.93	40.92	37.65	36.77
Henan	33.44	29.45	28.62	27.39	25.52	24.67
Hubei	24.48	20.85	20.07	19	17.43	16.64
Hunan	27.77	24.71	24.39	23.41	21.83	21.61
Guangdong	57.52	53.86	52.67	51.18	49	47.8
Guangxi	57.59	52.24	50.88	49.15	46.6	45.2
Hainan	15.64	14.23	13.88	13.48	12.94	12.62
Sichuan	72.24	61.37	59.15	56.2	52	49.86
Chongqing	9.21	7.64	7.3	6.87	6.23	5.91
Guizhou	36.08	30.57	29.48	27.83	25.35	24.23
Yunnan	96.96	83.73	81.35	77.18	71.1	68.69
Xizang	313.43	274.56	265.84	254.65	238.21	229.35
Shaanxi	29.28	24.64	23.78	22.44	20.44	19.57
Gansu	89.87	80.36	78.23	75.35	71.12	68.95
Qinghai	192.41	170.78	166.06	160	151.29	146.68
Ningxia	12.85	10.28	9.73	9.09	8.19	7.69
Xinjiang	370.6	319.58	308.76	293.71	271.51	260.79
Total	2169.32	1913.54	1860.48	1783.1	1668	1614.94

a) Reference concentration: 100 μg m^{-3}

Table 2 Atmospheric environmental capacities (10^4 t yr^{-1}) of SO_2, NO_2, NO_x, PM_{10}, $PM_{2.5}$ and NH_3 in mainland China

Recurrence interval (a)	Climate average	5	10	20	30	100
SO_2	1302	1148	1116	1070	1001	969
NO_2	868	765	744	713	667	646
NO_x	1085	957	930	892	834	807
PM_{10}	1519	1339	1302	1248	1168	1130
$PM_{2.5}$	759	670	651	624	584	565
NH_3	521	459	447	428	400	388

over, regional removal rates were increased under this isolated assumption (vs. actual cross-influence conditions). For example, the removal rate of Hebei Province increased 60% (from 3.813×10^5 rise to 6.12×10^5 t yr^{-1}).

When emission was arranged according to capacities calculated from climatic average removal rates, because annual average A-values were nearly normally distributed, approximately half the monitoring stations nationwide would exper-

Table 3 Removal rates (10^4 t yr^{-1}) in administrative regions of eastern China (3.74×10^6 km^2), ignoring impacts of pollutant emission from western China

Recurrence interval (a)	Climate average	5	10	20	30	100
Beijing	5.52	5.00	4.87	4.70	4.45	4.31
Tianjin	5.52	4.80	4.63	4.35	3.94	3.76
Hebei	61.16	54.80	53.55	51.31	47.82	46.40
Shanxi	51.60	45.26	43.99	42.36	39.94	38.68
Liaoning	67.84	62.62	61.19	58.86	55.22	53.66
Jilin	72.85	64.93	63.37	60.67	56.42	54.66
Heilongjiang	167.39	146.14	141.83	135.83	126.9	122.54
Shanghai	2.74	2.42	2.35	2.28	2.17	2.10
Jiangsu	34.36	30.08	30.38	29.10	26.86	27.88
Zhejiang	37.30	34.60	34.10	32.93	31.00	30.44
Anhui	38.08	32.03	30.95	28.99	26.00	24.88
Fujian	28.88	25.35	24.63	23.53	21.88	21.12
Jiangxi	33.53	28.19	27.07	25.55	23.33	22.22
Shandong	79.22	70.19	68.86	65.63	60.38	58.97
Henan	53.63	47.23	45.9	43.92	40.93	39.57
Hubei	39.26	33.44	32.18	30.48	27.96	26.69
Hunan	44.54	39.62	39.12	37.54	35.01	34.66
Guangdong	92.26	86.38	84.48	82.09	78.59	76.66
Guangxi	92.37	83.78	81.61	78.82	74.74	72.49
Hainan	25.08	22.82	22.26	21.63	20.76	20.24
Sichuan	115.85	98.42	94.87	90.14	83.40	79.97
Chongqing	14.77	12.25	11.70	11.02	9.99	9.48
Shaanxi	46.96	39.52	38.14	35.99	32.79	31.39
Total	1210.70	1069.9	1042.00	997.72	930.48	902.77

ience the events, i.e., annual average pollutant concentrations exceeding the standard limits. The recurrence-interval removal rates in Table 3 were calculated following the Pearson III type frequency distribution. In comparison, when capacities were calculated using removal rates at recurrence intervals 5, 30, and 100 yr, 20%, 3.3%, and 1% of the stations would have these events, respectively.

We also calculated annual removal rates per km^2, climatic averages, and at recurrence intervals 5–30 yr (Figure 3). Results showed that, in most of mainland China, 1–3 t of atmospheric pollutants could be removed over 1 km^2 of land. In the coastal region and western China, at least 2–4 t of pollutants could be removed over 1 km^2. In our calculations, mainland China was taken as the overall region, and the area of each sub-region was set to 1 km^2. Because the sub-regions in eq. (9) are additive, the removal rate for a region can be determined simply by multiplying its area with the local removal rate per km^2 (shown in Figure 3a). For example, for a 2×10^4 km^2 region near Beijing, the climatic average removal rate is estimated at 6×10^4 t yr^{-1}, and the removal rate at 30-year recurrence interval is about $3–4\times10^4$ t yr^{-1}. Therefore, data depicted in Figure 3a–d provide guideline information supporting regional planning of emission sources.

4. Estimation of daily removal rates at various recurrence intervals

Daily average A-values at recurrence intervals 7, 10, 20, 30, and 100 d were calculated similarly (Figure 3a–d). These results can be used to estimate daily removal rates and removal rate densities at various recurrence intervals, configure low-altitude emission sources, and control air quality under stable atmospheric conditions according to recurrence interval.

4.1 Distribution of daily average A-values at different recurrence intervals: topography and applications

Daily average A-values usually follow a positively skewed distribution (Xu et al., 2016). As a result, when the recurrence interval was prolonged, A-values in most regions of mainland China decreased rapidly. The decrease was relatively slow along the south coast of Guangdong and Guangxi provinces, because a lots of share of the atmospheric environmental ca-

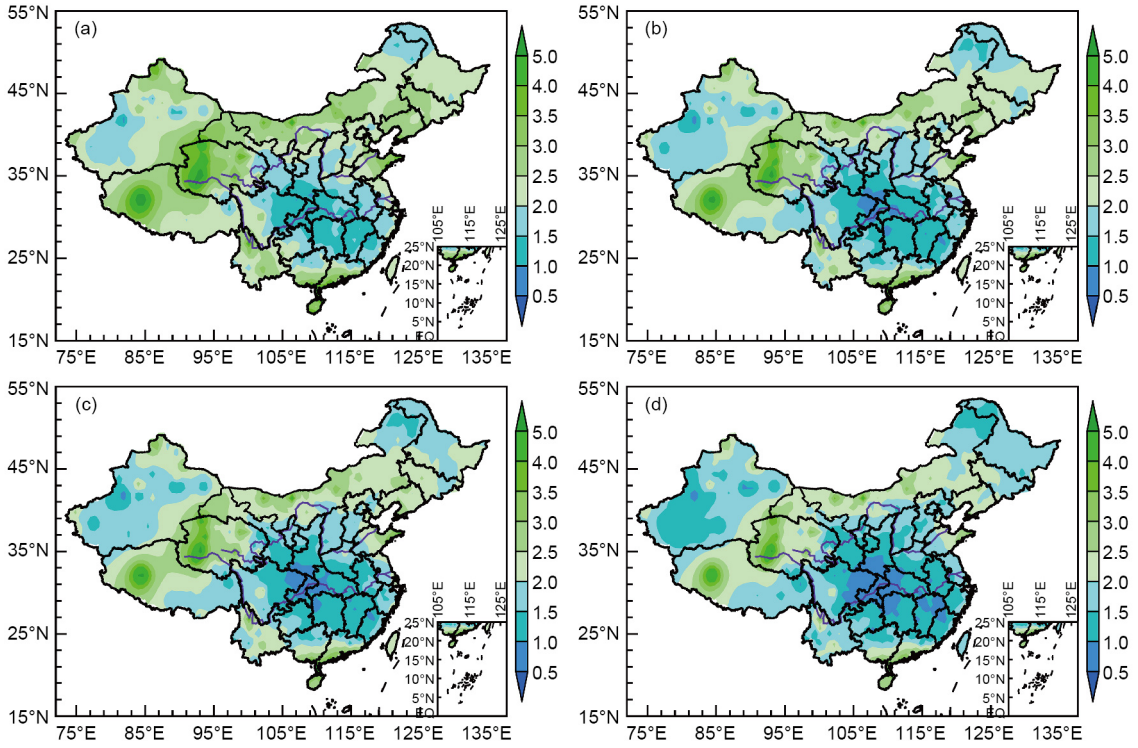

Figure 3 Annual removal rates at different recurrence interval (t km^{-2} a^{-1}). (a) Cimate average, (b) 5-year recurrence interval, (c) 10-year recurrence interval, (d) 30-year recurrence interval.

pacity in this region was attributed to dry and wet deposition. For this region, the left slope of the A-value distribution curve was flatter compared with areas in north China. Therefore, in this region, the A-value for a long recurrence interval (low probability) was greater than its counterpart value in northern China. For example (Figure 4c), the A-value at 30-day recurrence interval was 0.5–1 in Beijing, compared with 4–5 at the southern Guangdong-Guangxi coast, indicating that the latter has at least a 4-fold greater atmospheric environmental capacity than the former.

Averaged nationwide, A-values at recurrence intervals 7, 10, 20, 30, and 100 d were 36%, 26%, 15%, 13%, and 5% of climatic averages, respectively, as summarized in Table 4. Moreover (Figure 4b–d), A-values at recurrence intervals >20 d were largely <1.5, corresponding to atmospheric boundary layer thicknesses ~200 m or less. In this case, the atmospheric environmental capacity is dominated by A-values for low probability events, and may be used most effectively for managing low-altitude emission sources. During a low A-value (i.e., low-probability event) period, the capacity is typically controlled by the thickness of the stable boundary layer, and only low-altitude sources in the boundary layer affect air quality. In contrast, smoke plumes emitted from high-altitude sources are primarily above the stable boundary layer (i.e., residual layer) (Stull, 1988) and thus have only weak effects on the air below. The standard GB/T3840-91 requires that emissions from low-altitude sources account for 0.15–0.25 of total emission. It interesting that this range is similar to the ratios between daily average A-values at the above recurrence intervals and climate average values.

A small daily average A-value (low-probability event) occurs under light-wind or calm conditions. In this case, the effect of cross-regional airflows on the stable boundary layer is negligible, and removal rates for relatively isolated regions (cities) can be calculated by eq. (7) while ignoring large-scale, inter-regional interactions. In calculating atmospheric environmental capacities for a specific pollutant from its daily removal rates at various recurrence intervals, the daily standard average concentration limit should be used.

4.2 Estimation of daily removal rates at various recurrence intervals

Daily average A-values at different recurrence intervals were calculated for cities in mainland China by fitting to the Pearson type III distribution. Then, based on area percentages relative to their home provinces, removal rates (Table 4) of all mainland administrative regions were calculated via eq. (7) (C_r=100 μg m^{-3}).

Annualized daily removal rates of the regions (Table 4) were dependent on their local A-value distributions and territorial areas. In environmental planning, if regional emissions were regulated according to atmospheric environmental capacities in Table 1 or 3, and low-altitude emissions according to Table 4, air quality changes could theoretically be controlled through probability. For example, when low-altitude

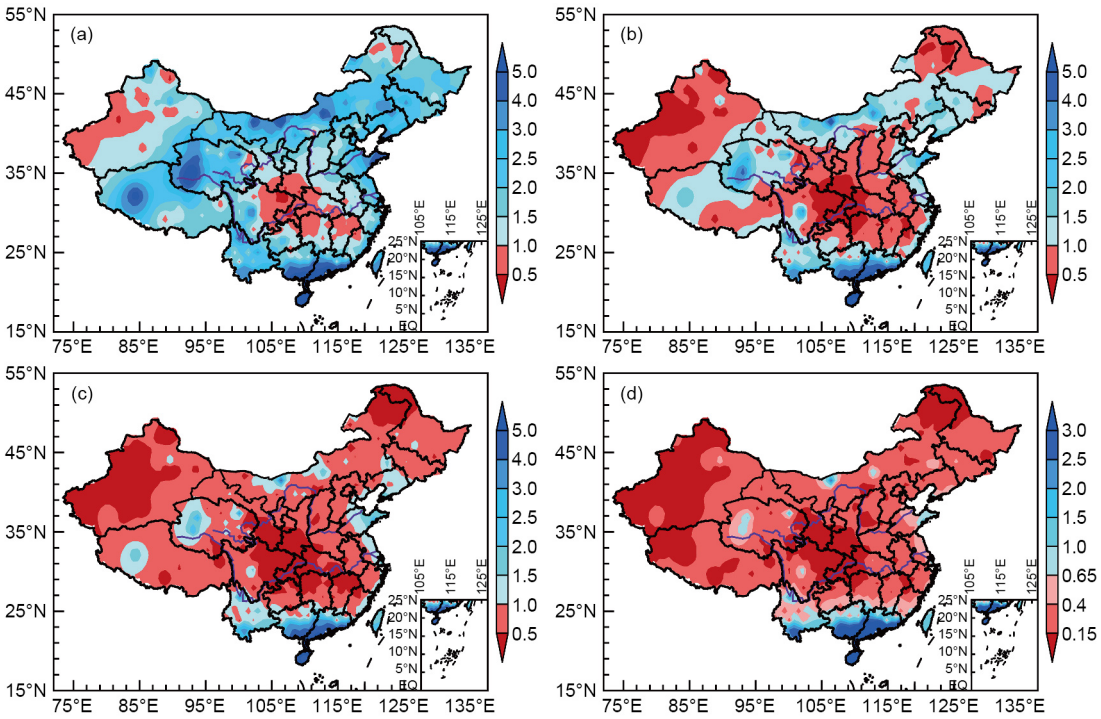

Figure 4 Distribution of daily average A-values at different recurrence interval. (a) 10-day recurrence interval, (b) 20-day recurrence interval, (c) 30-day recurrence interval, (d) 100-day recurrence interval.

emission sources are planned based on annualized daily removal rates at 7- and 100-day recurrence rates, air quality can generally meet the national standard 313 and 361 d each year, respectively. When total emission is controlled following Table 1 or 3 and low-altitude emission sources are not regulated according to Table 4, annual average air quality and the summer and spring qualities could theoretically be improved, whereas these qualities would not be improved effectively during the pollution-prone seasons.

4.3 Analyses of daily removal rate densities at various recurrence intervals

The removal rate density as defined in eq. (8) essentially describes the intensity of an pollution area source (or sink). Assuming that all low-altitude emission sources across mainland China could be modeled as one area source, daily removal rate densities at various recurrence intervals were calculated. The results are given in Table 5. However, this assumption is probably inappropriate. More reasonably, only built-up areas of a city (or urban agglomeration) may be appropriately regarded as emission area sources or unorganized emission sources. Therefore, we further analyzed the constraint of daily removal rates at different recurrent intervals on the size and change of built-up urban areas.

The size distribution of built-up urban areas of cities in mainland China were obtained from the *China City Statistical Yearbook 2014*. The distribution curve shows a peak at 20 km^2 (small and medium cities), another at 300 km^2 (large cities), and a minimum at 100 km^2 (Figure 5). Calculation of the reference removal rate densities suggests that for 100 km^2 as the reference area (S_r), acceptable air quality was ensured for most small and medium cities. Removal rates and densities for large cities were calculated from The following formula eq. (10) and their actual built area S. Figure 6a–d depict the distribution of removal rate densities at different recurrence intervals calculated at S_r=100 km^2. According to eq. (8), when A and C_r remain constant, the removal rate density for S (denoted Q_{ds}) can be converted from the removal rate density (Q_d) given in Figure 6a–d by

$$Q_{ds} = Q_d \times \sqrt{S_r / S}. \quad (10)$$

Calculations predicted that for a city ~100 km^2 in size, when it is regulated requiring that the low-altitude emission density not exceed removal densities at 10- or 100-day recurrence intervals (Figure 6a and d), it would have pollutant concentrations exceeding permissible levels on <37 or 3–4 d each year, respectively. Cities with built-up areas substantially larger than 100 km^2 were treated otherwise, as described below by the example of Beijing (built-up area S=1300 km^2). We calculated the removal rate density for $PM_{2.5}$ at 30-day recurrence interval. The permissible daily average $PM_{2.5}$ concentration (Grade 2 air quality standard) was selected as C_s=75 μg m^{-3}. It was observed (Figure 6c) that the removal rate density for Beijing was 5–10 kg h^{-1} km^{-2}, and the average (Q_d=7.5 kg h^{-1} km^{-2}) was used for calculation. The removal rate density for $PM_{2.5}$ ($Q_{dpm2.5}$) was thus calculated from eq. (10):

Table 4 Annualized daily removal rates (10^4 t yr^{-1}) of administrative regions of mainland China at different recurrence intervals[a)]

Recurrence interval (d)	7	10	20	30	100
Beijing	1.03	0.74	0.41	0.35	0.10
Tianjin	1.54	1.13	0.60	0.45	0.11
Hebei	12.54	9.22	5.28	4.63	1.42
Shanxi	9.80	7.07	3.90	3.39	0.93
Inner Mongolia	131.37	95.72	50.58	35.81	9.50
Liaoning	21.06	15.88	8.96	6.89	2.19
Jilin	17.15	12.27	6.37	4.32	1.21
Heilongjiang	37.26	26.55	13.79	13.23	2.66
Shanghai	0.81	0.66	0.46	0.41	0.20
Jiangsu	8.51	6.56	4.12	3.60	1.39
Zhejiang	11.56	9.05	5.50	4.44	1.45
Anhui	8.02	5.91	3.38	2.86	0.94
Fujian	6.36	4.86	3.01	2.67	0.99
Jiangxi	5.60	4.12	2.44	1.98	0.77
Shandong	22.73	17.65	10.89	9.94	3.23
Henan	10.92	7.92	4.38	3.83	1.06
Hubei	6.86	5.08	3.05	2.49	1.00
Hunan	7.50	5.46	3.14	2.57	0.89
Guangdong	34.44	31.47	27.71	25.68	22.38
Guangxi	29.33	26.25	22.54	20.89	17.91
Hainan	9.47	8.53	7.26	6.71	5.41
Sichuan	20.98	15.36	8.67	6.25	2.19
Chongqing	1.97	1.39	0.77	0.61	0.19
Guizhou	10.83	7.87	4.39	3.34	1.07
Yunnan	38.87	31.46	22.70	20.62	13.5
Tibet	109.45	72.70	30.80	30.06	3.66
Shaanxi	8.01	5.60	2.92	2.52	0.64
Gansu	27.01	19.25	10.35	9.07	2.26
Qinghai	70.63	50.75	26.65	20.35	5.53
Ningxia	3.73	2.59	1.33	1.15	0.26
Xinjiang	85.16	57.77	28.68	23.25	5.94
Total	770.50	566.84	325.03	274.36	110.98
Relative ratio to total climate average	0.36	0.26	0.15	0.126	0.05

a) Annualized daily removal rate=365×daily removal rate. Relative ratio to Total climate average 2.17×10^7 t yr^{-1} (Table 1)

Table 5 Nationwide average daily removal densities of mainland China at different recurrence intervals

Recurrence interval (d)	7	10	20	30	100
Nationwide removal rate (10^4 t yr^{-1})	770.5	566.84	325.03	274.36	110.98
Nationwide removal rate density (kg h^{-1} km^2)	0.091526	0.067334	0.03861	0.032591	0.013183

$$Q_{dpm2.5} = Q_d \times \sqrt{S_r / S} \times (C_s / C_r)$$
$$= 7.5 \times \sqrt{100 / 1300} \times \frac{75}{100}$$
$$= 1.56 \text{ kg h}^{-1} \text{ km}^{-2}.$$

Calculation also predicted that if the built-up area of Beijing expands from 100 to 1300 km^2, the removal rate density would decline by 72.3%. This example indicates that in the case of built-up area expansion, to prevent deterioration of air quality, unorganized emission density must be reduced proportionally following eq. (10) to match the reduced removal rate density. This may be done by controlling vehicle and

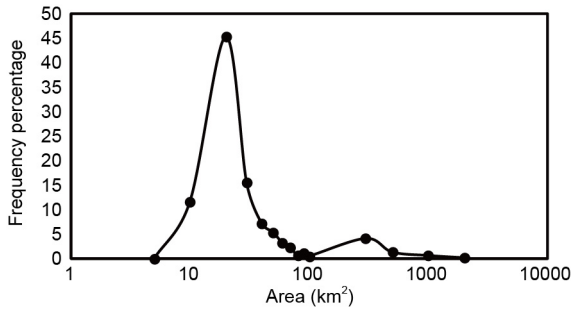

Figure 5 Frequency distribution of sizes of built-up areas of cities in mainland China.

population densities. Without such practices, the $PM_{2.5}$ concentration in Beijing would increase 3.6-fold after expansion.

5. Relationship between urban population density and atmospheric environment

5.1 Atmospheric environmental load vs. urban population density

Low climate average A-values (Figure 2a) were in densely populated regions. Economic effects followed population enrichment results to increase "agglomeration effects", leading to further population concentration and creating an escalating environmental load on the atmosphere. To quantitatively investigate the regional distribution of atmospheric environmental load in relation to local population, we defined an urban atmospheric load index as follows.

First, assuming that emissions from an urban unorganized source are proportional to population size, we can write $q_i = \alpha_i \times P_i$, where P_i is local population size and α_i the average emission per capita. According to eq. (7), under source-sink balance, the pollutant concentration in city i is $C_i = q_i / \left(A_i \times \sqrt{S_i}\right) = \alpha_i \times P_i / \left(A_i \times \sqrt{S_i}\right)$. Second, we conceptualized a "reference" city with average (of all i cities in the region of interest) population size $\overline{P}$, area $\overline{S}$, A-value $\overline{A}$, and emission per capita $\overline{\alpha}$. Then, the ratio between the pollutant concentration in a city of this region and that in the city was defined as the urban atmospheric load index of city i:

$$I_i = \frac{C_i}{\overline{C}} = \frac{P_i}{\overline{P}} \times \frac{\alpha_i}{\overline{\alpha}} \times \frac{\overline{A}}{A_i} \times \sqrt{\frac{\overline{S}}{S_i}}. \quad (11)$$

Figure 7 shows the distribution of population densities in cities of mainland China, calculated from data in China City Statistical Yearbook 2014. As of 2014, the nationwide average population density was 139 residents per km^2. Figure 8 shows the distribution of the index I_i across mainland China in winter, calculated using identical α_i Comparison of Figures 7 and 8 reveals that although the population density in the Sichuan Basin was not the highest in the country, it had the largest I_i, because it had the smallest A-values in mainland China. Consequently, improving the air quality in this region

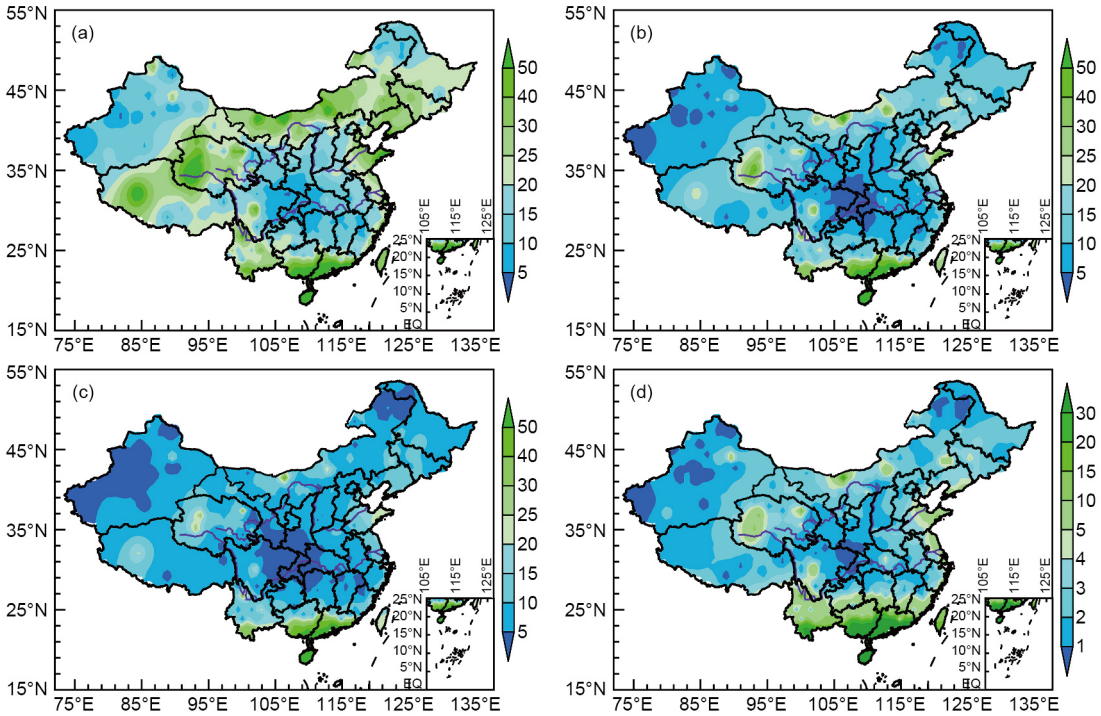

Figure 6 Distribution of hourly average reference removal rate densities at different recurrence interval (kg h^{-1} km^{-2}). (a) 10-day recurrence interval, (b) 20-day recurrence interval, (c) 30-day recurrence interval, (d) 100-day recurrence interval.

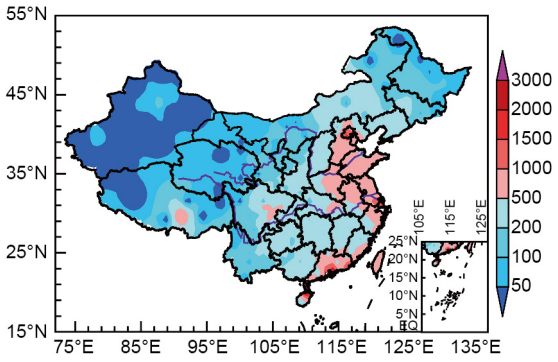

Figure 7 Distribution of population density (people km^{-2}).

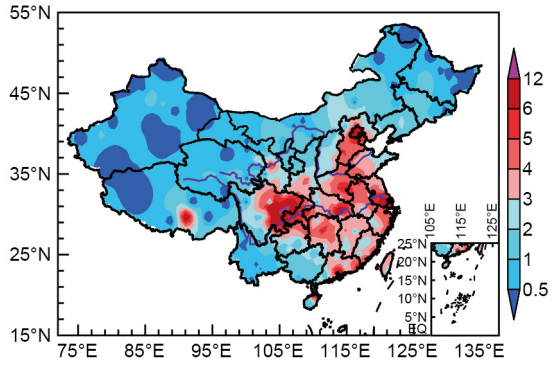

Figure 8 Distribution of urban atmospheric load indexes in winter.

is a challenging task that should be achieved by reducing regional α_i values according to the local population and A-values, as suggested by eq. (11). Large I_i also appeared in the Yangtze and Pearl river deltas. This was primarily because of their high population densities, as indicated by above-average A-values ($\overline{A}/A_i \leq 1$; Figure 2a) there. Accordingly, air quality control for these regions should aim to reduce the density of low-altitude emission sources. Moreover, the results show that in the region covering the Huang-Huai valleys and North China Plain, the impact of population density on the atmospheric environment was weaker than that on the Yangtze and Pearl river deltas. Thus, in case of severe pollution in that region, the cause can only be traced to strong local emissions per capita ($\alpha_i > \overline{\alpha}$). In fact, all large-index regions are considered pollution-prone. Western China had relatively low population densities (I_i<1), and air quality management in this large region should be quite feasible provided that the emission per capita does not greatly exceed the national average.

5.2 Impact of population concentration in built-up urban area on atmospheric environment

Given the current national population distribution, the impacts of hypothetical cities' dimension change on the atmospheric environment were simulated assuming that the current population of each city/town and emission rate per capita remain constant, and that the pollutant concentration has reached the reference level (100 μg m^{-3}; i.e., I_i=1). Four combinations of scenarios were simulated, i.e., all cities of ≥3 or ≥1 million local population were rescaled to give a density of 5000 or 10000 people km^{-2} (Wu et al., 2006; Dong and Wei, 2009). I_i for these scenarios were calculated from eq. (11) (Figure 9a–d). After these hypothetical changes, regions originally having high population densities were predicted to experience minor changes. In contrast, originally lightly populated regions (western China, Yunnan-Guizhou Plateau, and Guangxi-Hunan border) were expected to become new highly polluted areas, with I_i several-fold higher than the reference value. These results suggest that if urban development involves further population concentration, appropriate measures (i.e., reducing low-altitude emission rate) must be planned to prevent elevation of I_i.

Additionally, following eq. (11), when a city undergoes changes in dimension and population size, I_i can be calculated by eq. (12) using A-values at various recurrence intervals:

$$\frac{I_2}{I_1} = \frac{C_2}{C_1} = \frac{P_2}{P_1} \times \frac{\alpha_2}{\alpha_1} \times \frac{A_1}{A_2} \times \sqrt{\frac{S_1}{S_2}}, \tag{12}$$

where subscript 1 denotes quantities before the change, and 2 after.

If the city undergoes population concentration while I_i, A-values and population size remain constant, from eq. (12) we can write

$$\alpha_2 = \alpha_1 \times \sqrt{S_2/S_1}, \tag{13}$$

where S_1 and S_2 are residential areas before and after the population concentration, respectively. Eq. (13) indicates that under the above requirements, the emission rate per capita should be reduced by a factor of $\sqrt{S_2/S_1}$.

From eq. (12), the change of emission rate per capita (denoted I_e) for a city can be expressed by

$$I_e = \frac{\alpha_2}{\alpha_1} = \frac{P_1}{P_2} \times \frac{C_2}{C_1} \times \frac{A_2}{A_1} \times \sqrt{\frac{S_2}{S_1}}. \tag{14}$$

When the urban dimension and population size of the city remain constant, eq. (14) becomes

$$I_e = \frac{C_2}{C_1} \times \frac{A_2}{A_1}, \tag{15}$$

where the C- and A-values are averages from data recorded over the same period. I_e can be used to differentiate whether variation of pollutant concentrations in the atmosphere is primarily attributed to changes in emission rate or meteorological conditions. More specifically, I_e≈1 indicates variation caused predominantly by changes in atmospheric self-purification rate (effect of emission rate change is negligible). I_e<1 indicates variation caused by decreased emission rate, and I_e>1 indicates variation caused by increased emission rate.

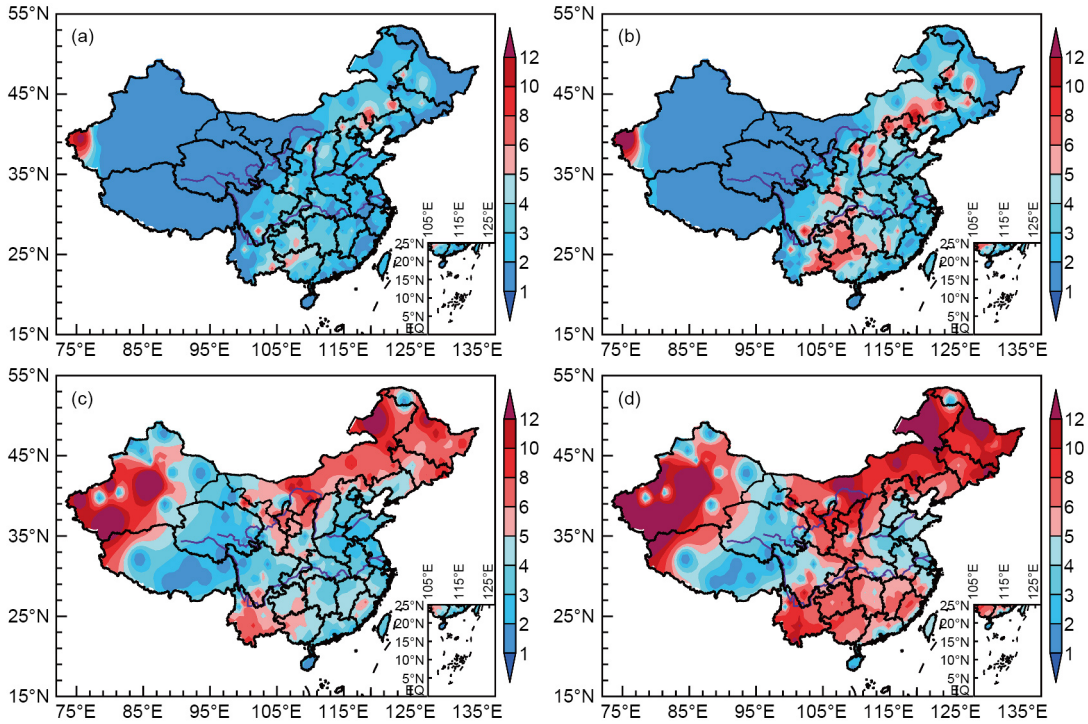

Figure 9 Distribution of urban atmospheric load indexes for different scenarios. (a) All regions of ≥3 million people are rescaled to 5000 people km^{-2}, (b) all regions of ≥3 million people are rescaled to 10000 people km^{-2}, (c) all regions of ≥1 million people are rescaled to 5000 people km^{-2}, (d) all regions of ≥1 million people are rescaled to 10000 people km^{-2}.

6. Discussion and conclusions

Under 100 μg m^{-3} reference pollutant concentration, the climatologically controlled removal rate of mainland China was found to be ~2.169×10^7 t yr^{-1}, and removal rates at 5–100 yr recurrence intervals were 1.913×10^7–1.615×10^7 t yr^{-1}. Nationwide, annualized removal rates at 10, 20, 30, and 100-day recurrence intervals in the stable boundary layer were 26%, 15%, 12.6%, and 5% of total annual removal rates, respectively. Corresponding atmospheric environmental capacities for target pollutants can be used to regulate low-altitude emission sources.

In urban planning, setting the smallest dimension of a city along the prevailing wind direction can effectively improve atmospheric transport/removal of pollutants, attaining maximum self-purification.

Urban expansion is accompanied by loss of removal rate density; if the built-up area is expanded from S_1 to S_2 and air quality is required to remain constant, the emission rate density of low-altitude emission sources should be reduced by a factor of $\sqrt{S_1/S_2}$.

During urbanization, increasing population density augments the emission rate density. However, to prevent air quality deterioration in the face of increased population density, I_i before and after the density change should be calculated, and measures must be adopted to prevent increase of the index. For example, if population size remains constant and residential area shrinks from S_1 to S_2, the emission rate per capita should be reduced by a factor of $\sqrt{S_2/S_1}$.

In interpreting changes of emission rate based on monitored pollutant concentrations, meteorological factors should be considered. For this purpose, change of emission rate per capita (I_e), as defined in eq. (15), may be used as an indicator.

A number of parameters were incorporated in calculations of A-values and removal rates, such as atmospheric boundary layer thickness, washout ratio, and dry deposition speed. Of these, boundary layer thickness appeared to be a critical in determining atmospheric environmental quality. With advancing field measurements and experimental studies, progressive improvement is expected for characterizing that thickness. Monitored data for various pollutants, cross-validation of data from various locations, and optimized deposition parameters may be incorporated in analyses to improve the accuracy of results and generate more valuable information for a region of interest.

Finally, for more complete estimation of atmospheric environmental capacities considering chemical conversion processes, the approach reported herein may be used to calculate an initial precursor distribution field. Subsequently, multi-source chemical-conversion modeling coupled to optimization methods including constraints (e.g., minimum increment/decrement, permissible secondary pollutant concentration) may be used to determine a more accurate capacity with consideration of secondary pollution.

Acknowledgements *This study was supported by the National Natural Science Foundation of China (Grant No. 41405136).*

References

An X Q, Chen Y C, Lu S H. 2004. Study on SO_2 atmospheric environment capacity in Lanzhou winter. Plateau Meteorol, 23:110–115

Chamberlain A C. 1953. Aspects of the Travel and Deposition of Aerosol Clouds and Vapours. AERE HP/R1261.HMSO, London

Dong X F, Wei Y Q. 2009. Study on valley-city population capacity in Mid-western China-taking the representative city Lanzhou as an example. J Arid Land Resour Environ, 23: 1–7

Li C K, Pan Y X, Sun R Q. 1985. Air Pollution Meteorology and Application. Beijing: Meteorological Press. 377–378

Li L, Cheng S Y, Chen D S, Hao L B, Fu H L. 2010. A calculated methodology of atmospheric environmental capacity based on CMAQ and control strategy. Environ Sci Tech, 33: 162–166

National Bureau of Statistics, Department of Urban Socioeconomic Survey 2014. China Urban Statistical Yearbook 2014. Beijing: China Statistics Press

National Environmental Protection Agency (China). 1991. Handbook on the Methods for Atmospheric Pollutant Total Emission Control in Urban Area. Beijing: China Environmental Science Press

National Environmental Protection Agency (China). 1991. Technical methods for making local standards of Air Pollutants (GB/T3840-91). Beijing: China Standard Press

People's Republic of China Environmental Protection Industry Standard (HJ/T 2.2-93). 1993. Technology Guidelines for Environmental Impact Assessment (Atmosphere Environment). Beijing: China Standard Press

Qian Y D, Wang Q G. 2011. An integrated method of atmospheric environmental capacity estimation for large-scale region. China Environ Sci, 31: 504–509

Stull R B. 1988. An introduction to Boundary Layer Meteorology. Netherlands: Kluwer Academic Publishers. 2

Sun W, Chen F, Wang H, Cheng X Q, Xu N. 2015. Application of CALPUFF model on calculation of atmospheric environmental capacity for SO_2 in Hefei city. J Nanjing Univ Inform Sci Tech-Nat Sci Edn, 7: 343–350

Wu W H, Niu S W, He X Z, Zeng M M. 2006. A study on valley-city population capacity in western china—Taking Tianshui city as an example. Econ Geogr, 26: 614–618

Xiao Y, Mao X Q, Ma G H, Li Z. 2008. Atmospheric environmental capacity study based on ADMS model and linear programming. Res Environ Sci, 21: 13–16

Xu D H. 1987. Some statistical values of the parameters of the diagnostic formulae on the depth of atmospheric boundary layer. J Beijing Inst Meteorol. Beijing: China Meteorological Press. 72–79

Xu D H, Wang Y. 2013. Plume footprints analysis for determining the bearing capacity of atmospheric environment. Acta Sci Circumst, 33: 1734–1740

Xu D H, Wang Y, Zhu R. 2016. The atmospheric environmental capacity coefficient cumulative frequency curve fitting and its application. China Environ Sci, 36: 2913–2922

Xu D H, Zhu R, Pan Z T. 1990. The studies on standard of emission of SO_2 and dispersion model in cities. China Environ Sci, 10: 309–313

Xu D H, Zhu R. 1989. A study on the distribution of ventilation and rainout capacity in mainland China. China Environ Sci, 9: 367–374

Xu H, Ding J, Feng X F. 2010. Calculation and programming of regional atmospheric environmental capacity based on ADMS-Urban model. Acta Sci Natural Univ Nakaiensis, 43: 67–72

Xue W B, Fu F, Wang J N, He K B, Lei Y, Yang J T, Wang S X, Han B P. 2014. Modeling study on atmospheric environmental capacity of major pollutants constrained by $PM_{2.5}$ compliance of Chinese cities. China Environ Sci, 34: 2490–2496

Zilitinkevich S. 1972. On the determination of the height of the Ekman boundary layer. Bound-Layer Meteorol, 3: 141–145